کارگاه های آموزشی مرکز اطلاعات علمی جهاد دانشگاهی

کارگاه آنلاین مکالمه روزمره انگلیسی

کارگاه آنلاین آموزش استفاده از وب آو ساینس

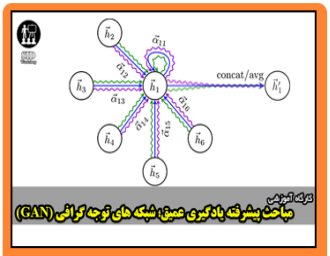

مباحث پیشرفته یادگیری عمیق؛
شبکه های توجه گرافی
(Graph Attention Networks)

Advances in Environmental Technology 2 (2015) 59-68

Advances in Environmental Technology

journal homepage: http://aet.irost.ir

Optimization and kinetic evaluation of acid blue 193 degradation by UV/peroxydisulfate oxidation using response surface methodology

Mojtaba Ahmadi*, Mohmmad Hamed Ardakani, ALi Akbar Zinatizadeh

Chemical Engineering Department, Faculty of Engineering, Razi University, Kermanshah, Iran

ARTICLE INFO

Article history:
Received 26 August 2014
Received in revised form
11 November 2015
Accepted 24 November 2015

Keywords:
Potassium peroxydisulfate
Blue dye
Response surface methodology
Color removal
Optimization

ABSTRACT

The optimization of process conditions for the degradation of Acid Blue 193 by UV/peroxydisulfate was investigated using response surface methodology (RSM). The effects of four parameters namely initial $K_2S_2O_8$ concentration, UV irradiation, temperature, and initial dye concentration on two process responses, color removal and the rate constants of the first-order kinetic equations, were investigated using a second-order polynomial multiple regression model. The analysis of variance (ANOVA) explained a high determination coefficient (R^2) value of 0.927-0.967, which ensures a good fit of the first-order regression model with the experimental data. The central composite design (CCD) was used to optimize the process conditions, which showed that an initial $K_2S_2O_8$ concentration of 5 mM, UV irradiation of 250 W, temperature of 50 °C, and the initial dye concentration of 40 mg/L were the best conditions. Under optimum conditions, the maximum color removal from the wastewater and the rate constants of the first-order kinetic equation were 100% and 0.086 min^{-1}, respectively.

1. Introduction

About 700,000 tons of dyes per year are produced worldwide. Nearly 10-15 percent of these dyes are discharged in effluent from dyeing operations [1]. Therefore, the decolorization of the colored effluent from dye industries is of vital importance before their release into the environment. Many conventional wastewater treatment methods such as chemical or electrochemical precipitation [2], biological oxidation [3, 4], biosorption [5], activated carbon adsorption [6-9], ozonation [10], and coagulation–flocculation [11] have been widely used to remove refractory pollutants from textile wastewaters [12]. Some of these processes are not very efficient because the dye compounds are hardly removed due to their resistance to biodegradation. However, these methods are not destructive and only transform the impurities in the solid state, and therefore the waste must be treated.

Biological oxidation is the most cost-effective process compared to the other treatments [13]. However, wastewater from the textile industry are known to contain harmful substances and/or non-biodegradable pollutants; therefore, conventional biochemical processes to treat solutions containing dyes and soluble biorefractory are inadequate [14].

Among the various treatment methods, advanced oxidation processes (AOPs) are considered as one of the most effective methods to degrade toxic pollutants and non-biodegradable organic pollutants [8, 14]. Among the advanced oxidation processes, the homogeneous AOPs employing peroxydisulfate [15-17] and UV/ peroxydisulfate [18-20] have been found to be very effective in the degradation of dye and pollutants.

Acid Blue 193 dye is widely used for silk and wool as well as for leather dyeing. It was chosen as a model contaminant for our degradation studies because it contains aromatic rings that make it difficult to treat with

*Corresponding author. Tel: +98-8334283262
E-mail address: m_ahmadi@razi.ac.ir

traditional processes [21]. To date, various techniques, including adsorption on bentonite [22] , natural sepiolite [23], red pine sawdust [24], declorization by *Cladosporium cladosporioides* [25], and biosorption using ash prepared from cow dung, mango stone, parthenium leaves, and activated carbon [26] have been reported for sepration and/or degradtion of Acid Blue 193. The research of Vijay kumar et al. was conducted using fungus *Cladosporium cladosporioides* as a decolorizing microorganism for the mineralization of Acid Blue 193 in an aqueous solution. Under the best conditions, the fungus completely decolorized a waste concentration of 100 mg l^{-1} of Acid Blue 193 in 8 days. Rasoulifard et al. studied the decolorization of Acid Blue 25 by UV/$S_2O_8^{2-}$ [27]. Under optimum conditions, the maximum color removal efficiency was 95%. The decolorization and mineralization of synthesized Acid Blue 113 by the UV/persulfate advanced oxidation process was examined by Shu et al. [28]. Also, Shu et al. studied the decolorization of azo dye Acid blue 113 by the UV/Oxone process. Various operating parameters for the removal of dye have been studied [29]. The research of Akay et al. was conducted using the heterogeneous fenton process for mineralization of burazol blue ED [30]. Under optimized reaction conditions, 96% color and 75% COD removals were obtained.

To the best of our knowledge, no previous studies have been conducted on the degradation of acid blue 193 by UV/peroxydisulfate oxidation. This study was conducted to optimize the process parameters (initial dye concentration, $K_2S_2O_8$ concentration, UV irradiation, and temperature) of Acid Blue 193 degradation and its kinetic study by UV/peroxydisulfate oxidation with response surface methodology (RSM). In doing so, the degradation process of the contaminent was enhanced.

2. Materials and Methods

2.1. Chemical

Synthetic colored wastewater containing an organic model pollutant (Acid Blue 193), commonly used as a textile dye, was obtained from the Boyakhsaz Company, Iran. The other chemicals, Potassium peroxydisulfate ($K_2S_2O_8$), H_2SO_4, and NaOH, were of laboratory reagent grade (Merck Co., Germany) and used without further purification.

2.2. Experimental methods

Acid Blue 193 degradation experiments were conducted in a photoreactor (Fig1.). For the UV/peroxydisulfate process, irradiation was carried out with a 125 and 250 W (UV-C) mercury lamp (Philips, the Netherland), which was put above a batch photoreactor. The distance between the solution and UV source was adjusted according to the experimental conditions. The reactor was equipped with a water-flow jacket for regulating the temperature by means of an external circulating flow of a thermostat. Since the photocatalysis was sustained by a ready supply of dissolved oxygen, air was supplied to the reaction system at a constant flow-rate using a micro-air compressor.

Dilute solutions of sodium hydroxide and sulfuric acid were used for pH adjustment and the initial pH values were measured by a Metrohm 827 pH/LF portable pH/conductivity-meter, Schott Instruments GmbH, Mainz, Germany. The prepared solution was transferred to the reactor and after adjusting the temperature, the UV lamp was switched on to initiate the process. During the experiments, a mild aeration was kept for mixing the content and saturation with O_2. Samples (6 mL) were taken at regular time intervals. A maximum total sampling volume of 24 mL was withdrawn during each experimental run, which is not significant when compared with the solution volume.

2.3. Analysis

The concentration of Acid Blue 193 in solution at different times was obtained by measuring absorbance at a maximum absorption wavelength (574 nm); the calculation of the decolorization decay was obtained from the calibration curve prepared earlier. An UNICO (USA) UV spectrophotometer (model- 2001SUV, USA) was employed for absorbance measurements by using a quartz cell of path length 1 cm. The color removal efficiency (¦) was achieved by using the following formula:

$$¦\ (\%) = \frac{C_o - C_t}{C_t} \times 100 \qquad (1)$$

where C_o and C_t are the initial concentration and the concentration of Acid Blue 193 at reaction time t, respectively.

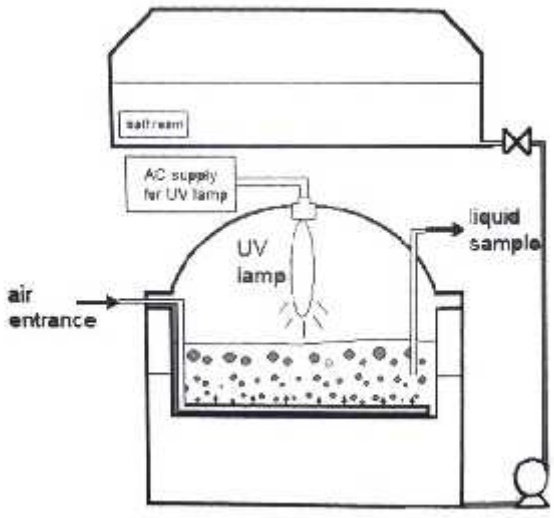

Fig. 1. The schematic view of the photo reactor set-up.

2.4. Kinetic modeling of the process

As a source of sulfate radicals, peroxydisulfate ($S_2O_8^{2-}$) has the advantages of high aqueous solubility and high stability at room temperature [15]. The reactions of peroxydisulfate

are generally slow at normal temperatures.The thermal or photochemical activated decomposition of $S_2O_8^{2-}$ ion to $SO_4^{\bullet-}$ radical has been proposed as a method of accelerating the process [31] and is summarized in the following reactions:

$$S_2O_8^{2-} + h^3 \rightarrow 2SO_4^{\bullet-} \quad (2)$$

$$SO_4^{\bullet-} + RH_2 \rightarrow SO_4^{2-} + H^+ + RH^{\bullet} \quad (3)$$

$$RH^{\bullet} + S_2O_8^{2-} \rightarrow R + SO_4^{2-} + H^+ + SO_4^{\bullet-} \quad (4)$$

$$SO_4^{\bullet-} + HR \rightarrow R^o + SO_4^{2-} + H^+ \quad (5)$$

$$2R^{\bullet} \rightarrow RR\,(\text{dimer}) \quad (6)$$

(R is an organic matter) In this oxidation process, sulfate ions will be generated as the end-product [32], which leads to a decrease in pH and an increase in salt content in the effluent. The SO_4^{2-} is practically inert and is not considered to be a pollutant. The USEPA has listed it under the secondary drinking water standards with a maximum concentration of 250 mg/L (1.43 mM), based on aesthetic reasons such as taste and odor [33].

In the present study, first and second-order reaction kinetics was used to study the decolorization kinetics of Acid Blue 193 by the UV/peroxydisulfate process. The individual expression was presented as below:

First-order reaction kinetics:

$$\frac{dC}{dt} = -k_1 C \quad (7)$$

By integrating the equation (7), the following equations could be obtained:

$$C_t = C_o \cdot \exp(-k_1 t) \quad (8)$$

where,

C_t: The concentration of RY84 at reaction time t (mM)

C_o: The initial concentration of the RY84 (mM)

k_1: The rate constant of the first-order kinetic equation (min^{-1})

2.5. Experimental design and data analysis

A central composite design (CCD) was employed in order to optimize the dye removal. Four factors were considered: initial $K_2S_2O_8$ concentration, UV irradiation, temperature, and initial dye concentration. Table 1 summarizes the levels for each factor involved in the design strategy. Table 2 shows the standard array for three factors and 26 experiments. It also shows the run order and the observed responses. The obtained model was evaluated for each response function and the experimental data (the color removal and the rate constants of the first-order kinetic equations) were analyzed statistically applying an analysis of variance (ANOVA).

The design consists of three series of experiments: (i) a two-level full factorial design 2^4 (all possible combinations of codified values +1 and –1); (ii) two central, replicates of the central point (0); and (iii) eight axial located at the center and both extreme levels of the experimental models [34].

Table 1. Independent variables and their levels in the central composite design used in the present study.

Parameter name	Code	Low (–1)	High (+1)
Initial $K_2S_2O_8$ concentration, mM	X_1	1	5
UV, W	X_2	0	250
Temperature, °C	X_3	10	50
Initial dye concentration, mg/L	X_4	40	200

$$y = \beta_0 + \sum_{j=1}^{k} \beta_j X_j + \sum_{j=1}^{k} \beta_{jj} X_j^2 + \sum_{j<j}^{k} \sum_{j=2}^{k} \beta_{ij} X_i X_j \quad (9)$$

where β_0, β_i, β_{ii}, and β_{ij} are the regression coefficients for intercept, linear, quadratic, and interaction terms, respectively; and X_i and X_j are the independent variables. The "Design expert" (version 7) was used for regression and graphical analyses of the obtained data.

3. Results and Discussion

3.1. Development of mathematical models

Design-Expert software was used for the analysis of the measured responses and determining the mathematical models with the best fits. The adequacy of the model was tested using the sequential f-test, lack-of-fit test, and the analysis-of-variance (ANOVA) technique using the same software to obtain the best-fit model

3.2. Analysis of color removal

The fit summary for color removal suggests a quadratic relationship where the additional terms are significant and the model is not aliased. The ANOVA table of the quadratic model with other adequacy measures R^2, adjusted $R^{2,}$ and predicted R^2 and are given in Table 3. The associated p-value of less than 0.05 for the model (i.e., α=0. 05, or 95% confidence level) indicates that the model terms are statistically significant. The lack-of-fit value of the model indicates non-significance, as this is desirable. The ANOVA result shows that the initial $K_2S_2O_8$ concentration, UV irradiation, temperature, initial dye concentration, and quadratic effect of the UV irradiation along with the interaction effect of the initial $K_2S_2O_8$ concentration and initial dye concentration and UV irradiation and temperature were the significant model terms associated with color removal. The other model terms were not significant, and thus eliminated by a backward elimination process to improve model adequacy.

Table 2. Factorial experimental design for treatment of dye by AOP.

Experiments no.	Initial $K_2S_2O_8$ concentration (X_1)	UV, W (X_2)	Temperature, ^oC (X_3)	Initial dye concentration (X_4)	Color removal	K_1 min^{-1}
1	-1	-1	-1	-1	11.76	0.001
2	1	-1	-1	-1	29.44	0.001
3	-1	1	-1	-1	96.12	0.025
4	1	1	-1	-1	99.96	0.076
5	-1	-1	1	-1	38.46	0.001
6	1	-1	1	-1	65.00	0.005
7	-1	1	1	-1	99.57	0.065
8	1	1	1	-1	99.60	0.092
9	-1	-1	-1	1	2.19	0.0001
10	1	-1	-1	1	19.15	0.001
11	-1	1	-1	1	46.47	0.005
12	1	1	-1	1	91.83	0.023
13	-1	-1	1	1	17.14	0.002
14	1	-1	1	1	52.47	0.004
15	-1	1	1	1	78.14	0.011
16	1	1	1	1	95.61	0.034
17	-1	0	0	0	89.10	0.021
18	1	0	0	0	97.20	0.03
19	0	-1	0	0	33.61	0.001
20	0	1	0	0	92.82	0.022
21	0	0	-1	0	91.64	0.02
22	0	0	1	0	97.27	0.025
23	0	0	0	-1	99.63	0.03
24	0	0	0	1	86.60	0.016
25	0	0	0	0	95.13	0.027
26	0	0	0	0	92.10	0.026

The ANOVA table for the reduced quadratic model is shown in Table 3. The reduced model results indicate that the model is significant (p-value less than 0.05). The other adequacy measures R^2, adjusted R^2, and predicted R^2 are in reasonable agreement and are close to 1, which indicate the adequacy of the model. The adequate precision compares the signal-to-noise ratio and a ratio greater than 4 is desirable. The value of the adequate precision ratio of 28.23 indicates an adequate model discrimination. The lack-of-fit f-value of 11.71 implies that the lack-of-fit is not significant relative to the pure errors [35].

The final mathematical models for color removal, which can be used for prediction within the same design space, are given as follows:

In terms of coded factors:

Color removal=93. 58+9.52X_1+29.49X_2+8.59X_3-8.33X_4+4.19 X_1X_4-4.50 X_2X_3-34.18 X_2^2

In terms of actual factors:

Color removal=17.92+1.62X_1+0.84X_2+0.65X_3-0.18X_4+0.026X_1X_4-1.8×$10^{-3}$$X_2X_3$-2.2×$10^{-3}$$X_2^2$

3.3. Analysis of the rate constants of the first-order kinetic equations

For the rate constants of the first-order kinetic equations, the fit summary recommends the quadratic model where the additional terms are significant and the model is not aliased. Table 4 presents the ANOVA table of the quadratic model with other adequacy measures R^2, adjusted R^2, and predicted R^2. The associated p-value of less than 0.05 (i.e. α=0. 05 or 95% confidence level) indicates that the model terms can be considered as statistically significant. The lack-of-fit value of the model indicates non-significance as desired. The analysis-of-variance result shows that the main effect of the initial $K_2S_2O_8$ concentration, UV

irradiation, temperature, and initial dye concentration along with the interaction effect of the initial $K_2S_2O_8$ concentration and UV irradiation, UV irradiation and temperature, UV irradiation, and initial dye concentration are the significant model terms associated with the rate constants of the first-order kinetic equations. The other model terms are not significant and are thus eliminated by a backward elimination process to improve model adequacy.

Table 3. ANOVA analysis of the color removal (after elimination).

Source	Sum of square	df	Mean square	*F*-value	*P*-value
Model	26940.47	7	3848.64	75.41	< 0.0001
Residual	918.68	18	51.04		
Lack of Fit	914.08	17	53.77	11.71	0.2263
Pure Error	4.59	1	4.59		
Total	27859.15	25			

R^2 = 96.70%; R^2 (adjust) = 95.42%; Adequate precision = 28.230. Coefficient of variation (CV) = 10.22%

Table 4. ANOVA analysis of the rate constants of the first-order kinetic equation.

Source	Sum of square	df	Mean square	F-value	P-value
Model	0.013117	7	0.001874	32.857	< 0.0001
Residual	0.001027	18	5.7E-05		
Lack of Fit	0.001026	17	6.04E-05	120.709	0.0715
Pure Error	5E-07	1	5E-07		
Total	0.014143	25			

R^2 = 92.74%; R^2 (adjust) = 89.92%; R^2 (predicted) = 83.3%; Adequate precision = 21.94. Coefficient of variation (CV) = 34.81%

The ANOVA table for the reduced quadratic model is presented in Table 4. The reduced model results indicate that the model is significant (p-value less than 0.05). The other adequacy measures R^2, adjusted R^2, and predicted R^2 are in reasonable agreement and are close to 1, which indicate an adequate model. The value of the adequate precision ratio 21.94 indicates adequate model discrimination. The lack-of-fit f-value of 120.71 implies that the lack-of-fit is not significant relative to the pure error [35].

The final mathematical models for the rate constants of the first-order kinetic equations, as determined by the Design Expert software, are given as follows:

In terms of coded factors:

$$K_1=0.022+7.5\times10^{-3}X_1+0.019X_2+4.8\times10^{-3}X_3-0.011X_4+7\times10^{-3}X_1X_2+4\times10^{-3}X_2X_3-0.012X_2X_4$$

In terms of actual factors:

$$K_1=4.13\times10^{-4}+2.44\times10^{-4}X_1+1.55\times10^{-4}X_2+4.11\times10^{-5}X_3+5\times10^{-6}X_4+2.8\times10^{-5}X_1X_2+1.6\times10^{-6}X_2X_3-1.2\times10^{-6}X_2X_4$$

3.4. Effects of process parameters on the responses

3.4.1. Color removal

Figure 2 is a perturbation plot which illustrates the effect of all the factors at the center point in the design space. It is apparent from this figure that the initial dye concentration has a negative effect on the color removal. This is because the rise in dye concentration induces an inner filter effect, and hence the solution becomes more and more impermeable to UV radiation [36]. It can also be observed from this plot that the initial $K_2S_2O_8$ concentration and temperature both have a minute positive effect on the color removal efficiency. These effects could be attributed to the following reason. An increase in the initial $K_2S_2O_8$ concentration increases the generation of sulfate radicals and hydroxyl radicals simultaneously and improves the decolorization of the dye [18, 19]. The results indicate that the color removal efficiency increases with the increase of UV radiation until it reaches its optimum value; the color removal then starts to decrease slightly as the UV radiation increases near the high limit.

The interaction effects of initial dye concentration and initial $K_2S_2O_8$ concentration on color removal are shown in Fig. 3 (a) and (b). These figures demonstrate that the color removal increases with decreasing initial dye concentration and increasing initial $K_2S_2O_8$ concentration. The experiments for the UV/$S_2O_8^{2-}$process showed that a 100% reduction of color occurred for the optimum conditions. Chang et al. showed that an overall degradation of 90% was achieved in 30 min for the photooxidation of iopromide by combined UV irradiation and peroxydisulfate [37]. This is due to the fact that an increase in the initial $K_2S_2O_8$ concentration results in an increase of the sulfate and hydroxyl radicals, and hence improves the photooxidation of the dye. The decolorization of the dye in the photooxidation process decreased with the increasing of the initial dye concentration. This was due to the fact that the higher dye concentration causes more absorption of UV light. In fact, an increase in the concentration of dye causes a rise of the internal optical density. Therefore, the solution is more impassable to UV light.

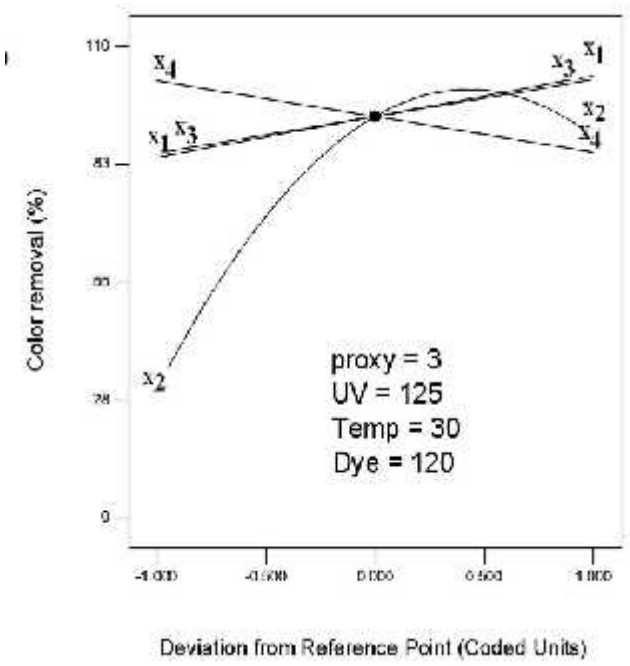

Fig. 2. Perturbation plot showing the effect of all factors on color removal.

Figure 4 (a) and (b) represent the interaction of UV and temperature on color removal. The UV radiation had a positive effect on the color decomposition. In the models for the color removal, x_2 was the major regressor variable affecting the responses (greatest coefficients, β_2=29. 49). In relation to the interaction of these two process parameters, the results indicated that increasing the UV up to the optimum value increased the color removal. Further, an increase of UV decreased the color removal. In this figure, it is evident that as the temperature increased, the color removal was increased.

3.4.2. The rate constants of the first-order kinetic equations

Figure 5 shows a perturbation plot to compare the effect of all the process parameters at the center point in the design space. From this figure, it can be observed that the rate constants of the first-order kinetic equations increases with the initial $K_2S_2O_8$ concentration. This was due to the fact that with an increase in initial $K_2S_2O_8$ concentration, the k_1 is increased. The result showed that the initial dye concentration has a negative effect on k_1, i.e., the decrease in the rate constants with increasing initial dye concentration has been observed. The presumed reason is from the effect of the higher dye concentration which causes more absorption of the UV light. Indeed, an increase in the dye concentration induces a rise in the medium optical density, and the solution therefore becomes more impermeable to the UV radiation. It can be observed from this plot that the rate constant varies positively with the UV radiation. Increasing the UV light increases the enhanced production of sulfate and hydroxyl radicals. At a low UV radiation, the rate of photolysis of $S_2O_8^{2-}$ is limited. However, at a high UV radiation, the formation of sulfate and hydroxyl radicals increases upon the photodissociation of $S_2O_8^{2-}$, and hence the constant rate of decolorization increases [19, 36]. The temperature contributes a slightly positive effect on the rate constant.

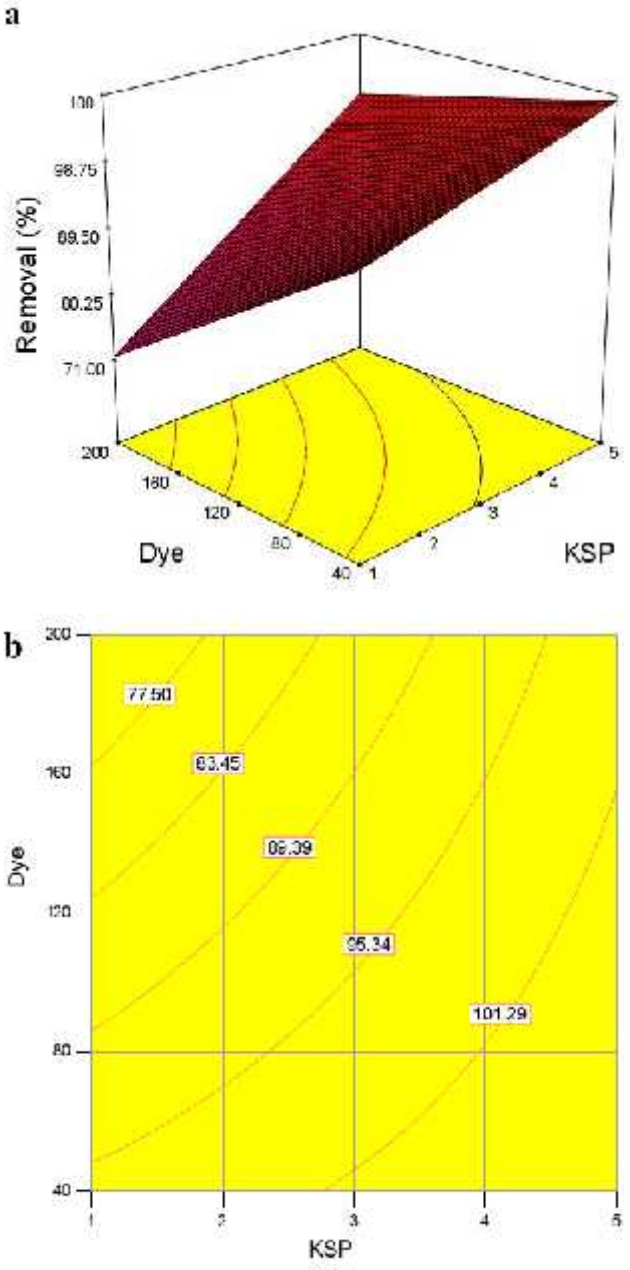

Fig. 3. (a) Response surface plot and (b) contours plot showing the effect of initial dye concentration (mg/l) and initial $K_2S_2O_8$ concentration (mM) on the color removal at UV=125 W and Temperature=30°C.

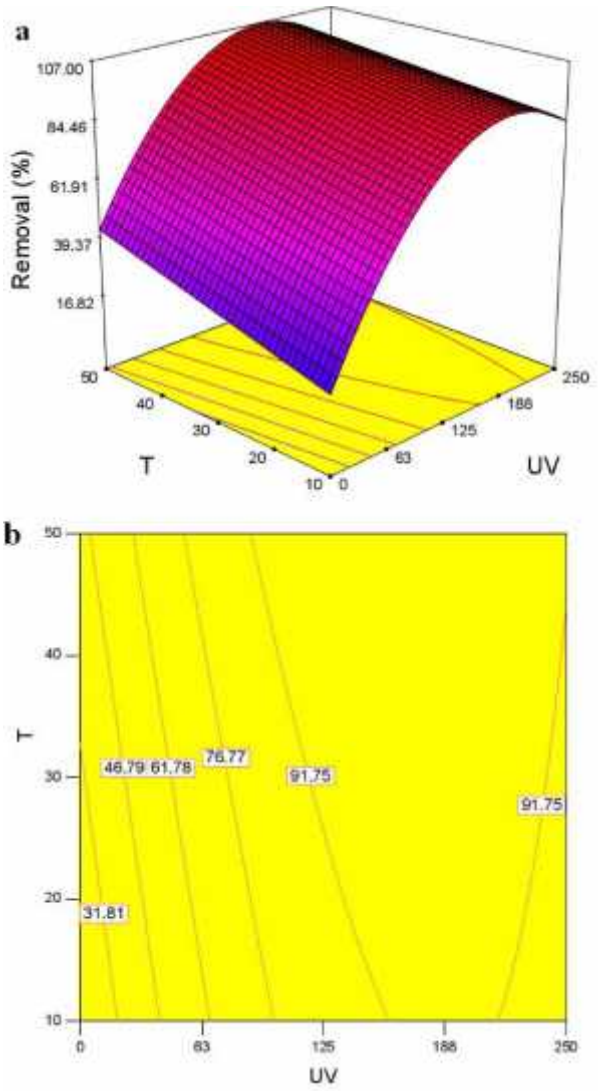

Fig. 4. (a) Response surface plot and (b) contours plot showing the effect UV (W) and temperature (30°C) on the color removal at an initial $K_2S_2O_8$ concentration 3mM and initial dye concentration 120mg/l.

Figure 6 (a) and (b) show the interaction effect of UV and initial $K_2S_2O_8$ concentration on the decolorization rate constant. From this figure, it is evident that as the UV and initial $K_2S_2O_8$ concentration increase, the decolorization rate constant also increases. This observation agrees with the results of other studies. It is reasonable to expect that by increasing the concentration of peroxydisulfate ion, more sulfate and hydroxyl radicals are available to attack the aromatic rings and the decolorization rate constant is increased [38]. Similar results were also obtained by former studies [39]. Khataee et al. investigated the decolorization of Basic Blue by UV/peroxydisulfate treatment. They described that an increase in the decolorization rate constant resulted in an increase in $S_2O_8^{2-}$ [18].

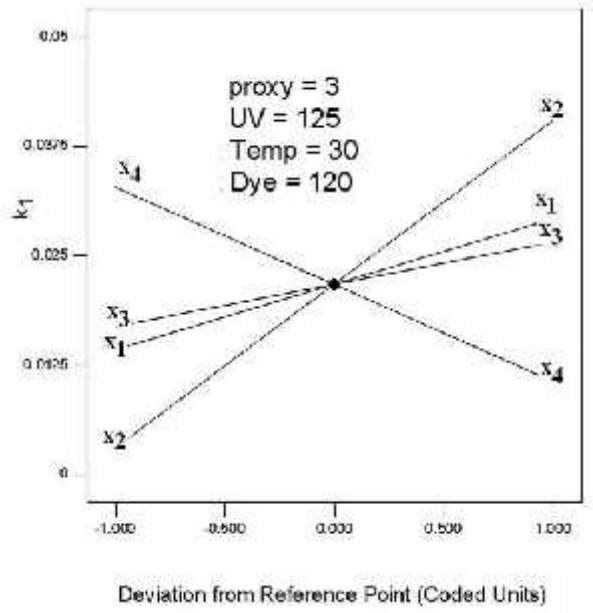

Fig. 5. Perturbation plot showing the effect of all factors on the K_1.

In the decolorization rate constant models, the UV radiation was the major regressor variable affecting the responses (greatest coefficients, β_2=0. 019). Figure 7 depicts the response surface plot showing the effect of UV and temperature on the decolorization rate constant at a fixed initial $K_2S_2O_8$ concentration (3 mM) and an initial dye concentration (120 mg/l). The results indicate that even at high UV levels, an increase in temperature at a fixed UV led to a marked increase in the decolorization rate constant. The present study shows that the decolorization rate constant could be increased with increasing the UV at all the levels of temperature. These results are significant in view of the earlier literature reports [40, 41]. At a higher temperature, the accelerated peroxydisulfate decolorization has been more effective which improved the generation rate of $^{\bullet}OH$, and therefore enhanced the decolorization of the dye [42].

The interaction effects of initial dye concentration and UV on the decolorization rate constant is shown in Fig. 8 (a) and (b). These figures demonstrate that the decolorization rate constant increases with decreasing initial dye concentration and increasing UV. The reason is the same as that stated earlier. A similar result was reported by Khatee et al. that found a decrease in photooxidative decolorization rate with increasing initial dye concentration [18].

4. Conclusions

The following conclusions can be drawn from this study based on the range of values of parameters considered.

1. Increasing initial $K_2S_2O_8$ concentration increases the color removal efficiency and the rate constants of the first-

order kinetic equations; whereas, increasing initial dye concentration decreases both the responses.

2. In the case of UV irradiation, the color removal increases with the UV irradiation until it reaches its closest to optimum value, the color removal then starts to drop as the UV irradiation is increased.

3. The rate constants of the first-order kinetic equations increases as the UV irradiation increases.

4. The temperature has a slight positive effect on the color removal efficiency.

5. The temperature contributes positively with a statistically significant effect on the rate constants of the first-order kinetic equations.

6. The optimum conditions for this treatment was achieved by setting the experiment with an initial $K_2S_2O_8$ concentration at 5 mM, the UV irradiation at 250W, and the temperature at 50 ^{o}C while the initial dye concentration level was at 40 mg/L.

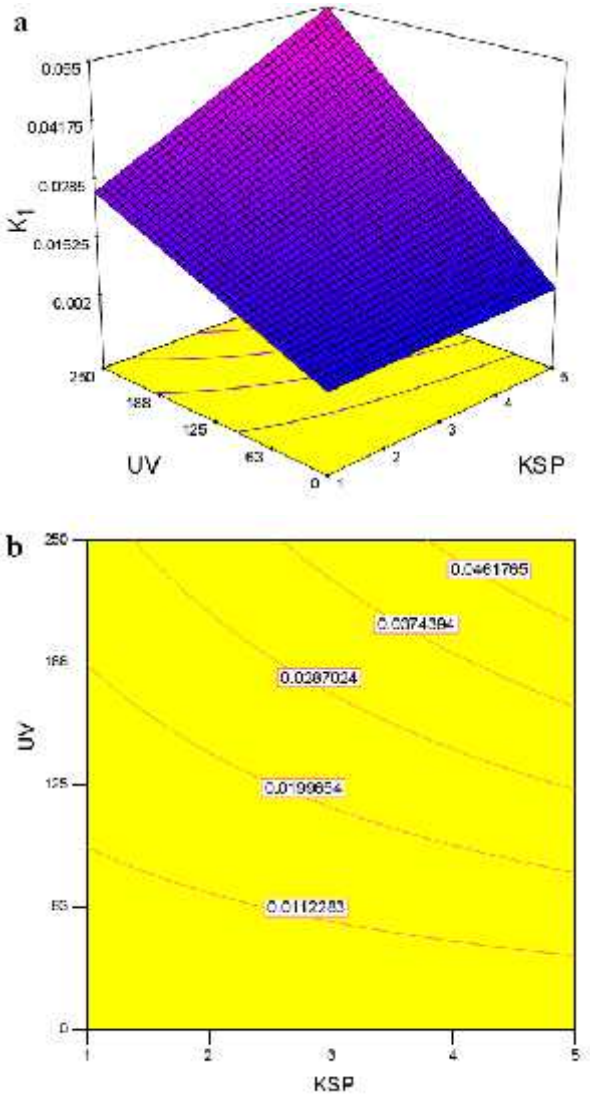

Fig. 6. (a) Response surface plot and (b) contours plot showing the effect of UV (W) and initial $K_2S_2O_8$ concentration (mM) on decolorization rate constant at initial dye concentration=120 mg/l and Temperature=30^{o}C.

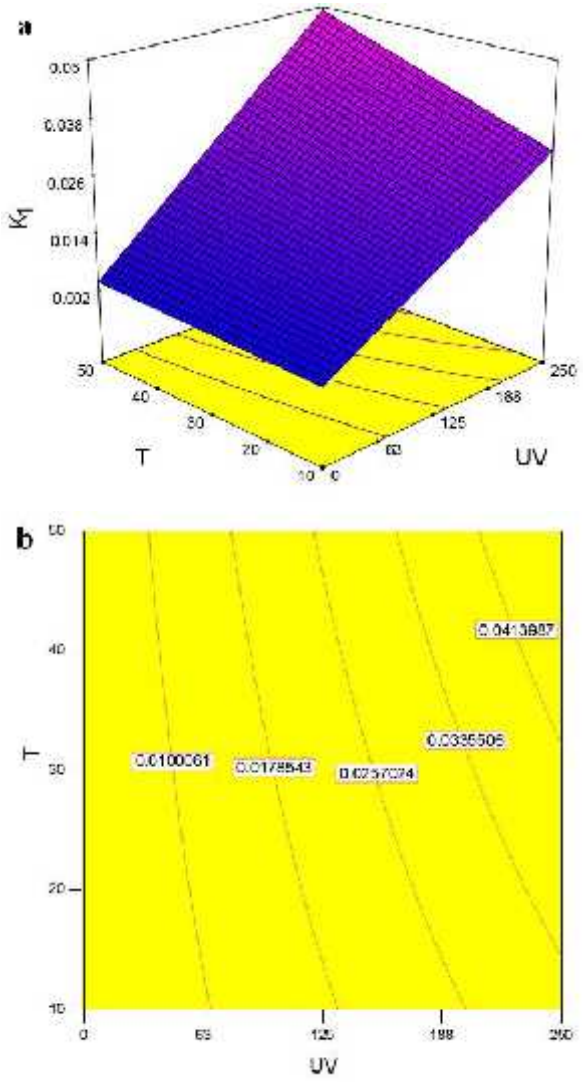

Fig. 7. (a) Response surface plot and (b) contours plot showing the effect of UV (W) and temperature (30^{o}C) on decolorization rate constant at initial $K_2S_2O_8$ concentration=3 mM and initial dye concentration=120 mg/l.

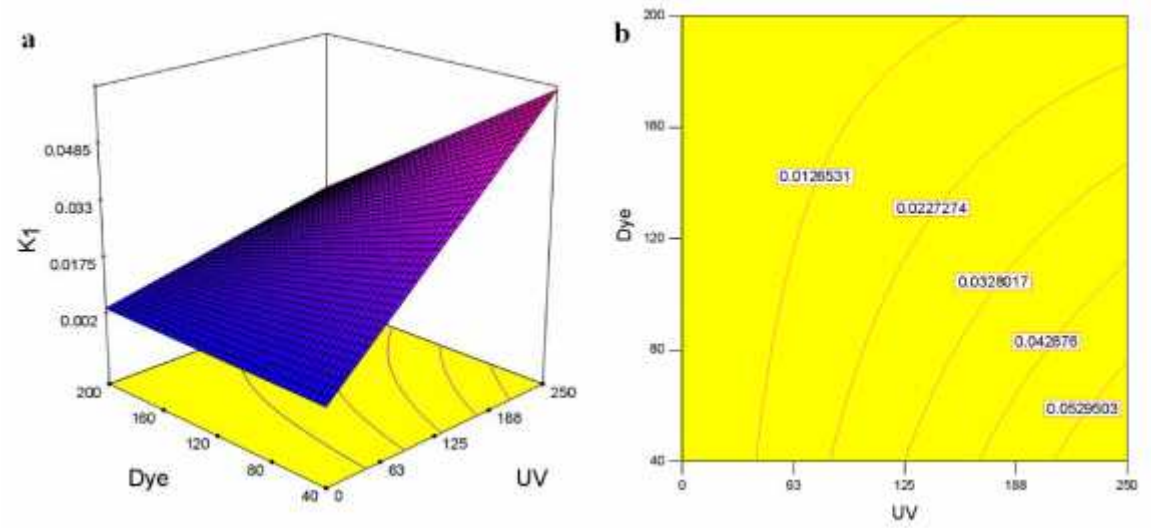

Fig. 8. (a) Response surface plot and (b) contours plot showing the effect of UV (W) and initial dye concentration (mg/L) on decolorization rate constant at initial $K_2S_2O_8$ concentration =3mM and Temperature=300^oC.

References

[1] Zollinger, H., (1991). Colour chemistry: Synthesis properties and application of organic dyes and pigments. New York VCH publishers.

[2] Fongsatitkul, P., Elefsiniotis, P., Boonyanitchakul, B. (2006). Treatment of a textile dye wastewater by an electrochemical process. *Journal of environmental science and health part A*, *41*(7), 1183-1195.

[3] Işık, M., Sponza, D. T. (2008). Anaerobic/aerobic treatment of a simulated textile wastewater. *Separation and purification technology*, *60*(1), 64-72.

[4] Pandey, B. V., & Upadhyay, R. S. (2006). Spectroscopic characterization and identification of pseudomonas fluorescens mediated metabolic products of Acid Yellow-9. *Microbiological research*, *161*(4), 311-315.

[5] Ranjusha, V. P., Pundir, R., Kumar, K., Dastidar, M. G., Sreekrishnan, T. R. (2010). Biosorption of remazol Black B dye (Azo dye) by the growing Aspergillus flavus. *Journal of environmental science and health Part A*, *45*(10), 1256-1263.

[6] Özacar, M., Şengil, I. A. (2003). Adsorption of reactive dyes on calcined alunite from aqueous solutions. *Journal of hazardous materials*, *98*(1), 211-224.

[7] Akkaya, G., Uzun, İ., Güzel, F. (2007). Kinetics of the adsorption of reactive dyes by chitin. *Dyes and pigments*, *73*(2), 168-177.

[8] Benkli, Y. E., Can, M. F., Turan, M., Celik, M. S. (2005). Modification of organo-zeolite surface for the removal of reactive azo dyes in fixed-bed reactors. *Water research*, *39*(2), 487-493.

[9] Geethakarthi, A., & Phanikumar, B. R. (2011). Adsorption of reactive dyes from aqueous solutions by tannery sludge developed activated carbon: Kinetic and equilibrium studies. *International journal of environmental science & technology*, *8*(3), 561-570.

[10] Lin, S. H., Liu, W. Y. (1994). Treatment of textile wastewater by ozonation in a packed-bed reactor. *Environmental technology*, *15*(4), 299-311.

[11] Kashefialasl, M., Khosravi, M., Marandi, R., Seyyedi, K. (2006). Treatment of dye solution containing colored index acid yellow 36 by electrocoagulation using iron electrodes. *International journal of environmental science and technology, 2*(4), 365-371.

[12] Daneshvar, N., Sorkhabi, H. A., Kasiri, M. B. (2004). Decolorization of dye solution containing Acid Red 14 by electrocoagulation with a comparative investigation of different electrode connections. *Journal of hazardous materials*, *112*(1), 55-62.

[13] Metcalf & Eddy (Empresa comercial). (1991). *Wastewater Engineering: Treatment disposal and reuse*. Irwin Mcgraw Hill.

[14] Ternes, T. A., Hirsch, R. (2000). Occurrence and behavior of X-ray contrast media in sewage facilities and the aquatic environment. *Environmental science & technology*, *34*(13), 2741-2748.

[15] Xu, X. R., Li, X. Z. (2010). Degradation of azo dye Orange G in aqueous solutions by persulfate with ferrous ion. *Separation and purification technology*, *72*(1), 105-111.

[16] Rastogi, A., Al-Abed, S. R., Dionysiou, D. D. (2009). Sulfate radical-based ferrous–peroxymonosulfate oxidative system for PCBs degradation in aqueous and sediment systems. *Applied catalysis B: environmental*, *85*(3), 171-179.

[17] Wang, P., Yang, S., Shan, L., Niu, R., Shao, X. (2011). Involvements of chloride ion in decolorization of Acid Orange 7 by activated peroxydisulfate or

peroxymonosulfate oxidation. *Journal of environmental sciences*, *23*(11), 1799-1807.

[18] Khataee, A. R., Mirzajani, O. (2010). UV/peroxydisulfate oxidation of CI Basic Blue 3: Modeling of key factors by artificial neural network. *Desalination*, *251*(1), 64-69.

[19] Salari, D., Niaei, A., Aber, S., Rasoulifard, M. H. (2009). The photooxidative destruction of CI Basic Yellow 2 using UV/$S_2O_8^{2-}$ process in a rectangular continuous photoreactor. *Journal of hazardous materials*, *166*(1), 61-66.

[20] Zhang, H., Zhang, J., Zhang, C., Liu, F., Zhang, D. (2009). Degradation of CI acid 0range 7 by the advanced Fenton process in combination with ultrasonic irradiation. *Ultrasonics sonochemistry*, *16*(3), 325-330.

[21] Panizza, M., Cerisola, G. (2009). Electro-Fenton degradation of synthetic dyes. *Water research*, *43*(2), 339-344.

[22] Özcan, A. S., Erdem, B., Özcan, A. (2004). Adsorption of Acid Blue 193 from aqueous solutions onto Na–bentonite and DTMA–bentonite. *Journal of colloid and Interface science*, *280*(1), 44-54.

[23] Özcan, A., Öncü, E. M., Özcan, A. S. (2006). Kinetics, isotherm and thermodynamic studies of adsorption of Acid blue 193 from aqueous solutions onto natural sepiolite. *Colloids and surfaces A: Physicochemical and engineering aspects*, *277*(1), 90-97.

[24] Can, M. (2015). Investigation of the factors affecting acid blue 256 adsorption from aqueous solutions onto red pine sawdust: equilibrium, kinetics, process design, and spectroscopic analysis. *Desalination and water treatment*, (DOI: 10.1080/19443994.2014.1003974).

[25] Vijaykumar, M. H., Veeranagouda, Y., Neelakanteshwar, K., Karegoudar, T. B. (2006). Decolorization of 1: 2 metal complex dye Acid blue 193 by a newly isolated fungus, Cladosporium cladosporioides. *World journal of microbiology and biotechnology*, *22*(2), 157-162.

[26] Purai, A., & Rattan, V. K. (2012). Biosorption of leather Dye (Acid Blue 193) from aqueous solution using ash prepared from cow dung, mango stone, parthenium leaves and activated carbon. *Indian chemical engineer*, *54*(3), 190-209.

[27] Rasoulifard, M. H., Fazli, M., Inanlou, M., Ahmadi, R. (2015). Evaluation of the effectiveness of process in removal trace anthraquinone CI acid blue 25 from wastewater. *Chemical engineering communications*, *202*(4), 467-474.

[28] Shu, H. Y., Chang, M. C., Huang, S. W. (2015). UV irradiation catalyzed persulfate advanced oxidation process for decolorization of Acid Blue 113 wastewater. *Desalination and water treatment*, *54*(4-5), 1013-1021.

[29] Shu, H. Y., Chang, M. C., Huang, S. W. (2015). Decolorization and mineralization of azo dye Acid Blue 113 by the UV/Oxone process and optimization of operating parameters. *Desalination and Water Treatment*, (DOI: 10.1080/ 19443994.2015.1031188).

[30] Akay, U., Demirtas, E. A. (2015). Degradation of burazol blue ED by heterogeneous fenton process: simultaneous optimization by central composite design. *Desalination and water treatment*, 56(12), 3346-3356.

[31] House, D. A. (1962). Kinetics and mechanism of oxidations by peroxydisulfate. *Chemical reviews*, *62*(3), 185-203.

[32] Maurino, V., Calza, P., Minero, C., Pelizzetti, E., Vincenti, M. (1997). Light-assisted 1, 4-dioxane degradation. *Chemosphere*, *35*(11), 2675-2688.

[33] Weiner, E. R. (2000). A Dictionary of inorganic water quality parameters and pollutants. *Applications of environmental chemistry, A practical guide for environmental professionals*, 27.

[34] Lapin, L. L. (1997). *Modern engineering statistics*. Duxbury.

[35] Vining, G. G., Kowalski, S. (2010). *Statistical methods for engineers*. Cengage Learning.

[36] Modirshahla, N., Behnajady, M. A., Ghanbary, F. (2007). Decolorization and mineralization of CI Acid Yellow 23 by Fenton and photo-Fenton processes. *Dyes and pigments*, *73*(3), 305-310.

[37] Chan, T. W., Graham, N. J., Chu, W. (2010). Degradation of iopromide by combined UV irradiation and peroxydisulfate. *Journal of hazardous materials*, *181*(1), 508-513.

[38] Oh, S. Y., Kim, H. W., Park, J. M., Park, H. S., Yoon, C. (2009). Oxidation of polyvinyl alcohol by persulfate activated with heat, Fe 2+, and zero-valent iron. *Journal of hazardous materials*, *168*(1), 346-351.

[39] Sun, S. P., Li, C. J., Sun, J. H., Shi, S. H., Fan, M. H., Zhou, Q. (2009). Decolorization of an azo dye Orange G in aqueous solution by Fenton oxidation process: Effect of system parameters and kinetic study. *Journal of hazardous materials*, *161*(2), 1052-1057.

[40] Lau, T. K., Chu, W., Graham, N. J. (2007). The aqueous degradation of butylated hydroxyanisole by UV/$S_2O_8^{2-}$: study of reaction mechanisms via dimerization and mineralization. *Environmental science & technology*, *41*(2), 613-619.

[41] Kasiri, M. B., Khataee, A. R. (2011). Photooxidative decolorization of two organic dyes with different chemical structures by UV/H 2 O 2 process: experimental design. *Desalination*, *270*(1), 151-159.

[42] Sun, S. P., Li, C. J., Sun, J. H., Shi, S. H., Fan, M. H., Zhou, Q. (2009). Decolorization of an azo dye Orange G in aqueous solution by Fenton oxidation process: Effect of system parameters and kinetic study. *Journal of hazardous materials*, *161*(2), 1052-1057.

کارگاه های آموزشی مرکز اطلاعات علمی جهاد دانشگاهی

کارگاه آنلاین مکالمه روزمره انگلیسی

کارگاه آنلاین آموزش استفاده از وب آو ساینس

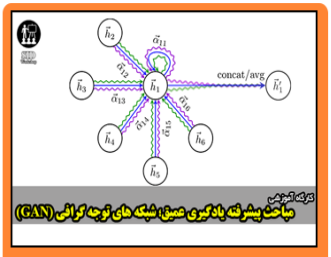

مباحث پیشرفته یادگیری عمیق؛ شبکه های توجه گرافی (Graph Attention Networks)